Comparison of experimental and predicted divertor fluxes in W7-X scraper element mimic scenarios

J.D. Lore[1*], Y. Gao[2], H. Niemann[3], T. Barbui[4], P. Drewelow[3], G. Wurden[5], J. Geiger[3], M. Jakubowski[3], and the W7-X team[3]

[1] *Oak Ridge National Laboratory, Oak Ridge, USA*

[2] *Forschungzentrum Juelich, Juelich, Germany*

[3] *Max Planck Institute for Plasma Physics, Greifswald, Germany*

[4] *University of Wisconsin-Madison, Madison, WI, USA*

[5] *Los Alamos National Laboratory, Los Alamos, NM, USA*

Introduction: The scraper element (SE) [1, 2] is a divertor component designed to protect low-rated areas of the primary divertor in the Wendelstein 7-X (W7-X) stellarator in certain scenarios. The scenarios predicted to result in overload are high power, long-pulse plasmas where the net toroidal current evolves to ~43 kA over ~100 seconds [3]. These conditions are not available until the actively cooled operational phase of the device (OP2). In order to verify the key physics aspects of the SE, special magnetic configurations were developed to mimic the effect of the toroidal current and plasma beta evolution on the divertor flux patterns using the W7-X coil set [4]. Experiments were performed in the first diverted operational phase (OP1.2a) of W7-X without SEs installed to assess the heat and particle fluxes to the divertor components. The primary goals were to confirm the validity of mimicking otherwise inaccessible plasma conditions in vacuum magnetic configurations, and that the flux patterns on the divertor were as predicted. Here we focus on comparison of the divertor heat fluxes measured by infrared cameras [5] to rapid field line diffusion calculations using the DIV3D code used to design the SE [2,6]. Two adiabatically cooled SEs have been installed in the machine in preparation for the next experimental campaign (OP1.2b). Companion experiments to the ones discussed here are planned to confirm the protection of the primary divertor edges and assess any side effects of the SE, such as a reduction in pumping efficiency and additional recycling source.

Experimental setup: The OP2 scenario predicted to result in overload has a steady-state toroidal current of ~43kA. In order to achieve acceptable fluxes in steady-state, the vacuum rotational transform is reduced such that the final configuration has the 5/5 island chain in the edge, and the heat fluxes are predicted to be in acceptable stripe patterns away from the low rated edges along the pumping gap. During the design of the SE, five points along this evolution were studied, with magnetic equilibria corresponding to five toroidal currents: 0kA, 11kA, 22kA, 32kA, and 43kA. The 22kA and 32kA configurations are predicted to result in overload conditions in OP2. Similarly, five mimic configurations were designed to reproduce the important features of the divertor flux patterns. The same 0kA to 43kA labels are used to refer to these configurations, even though they are designed to have the desired topology in vacuum. Although no SEs were installed in OP1.2a, the thermal properties of the adiabatically cooled SE set an upper limit on the input power and pulse length. The reference discharge planned for OP1.2b operation in the mimic configurations is 6.25s, with P_{in} = 2MW. This reference input power was used in all five mimic configurations during OP1.2a, with shots corresponding to working gasses of Helium and Hydrogen in each case. In the critical 22kA and 43kA configurations density and power scans were performed. Here we limit the discussion to a set of five pulses with Hydrogen working gas and 2MW of input power, see Fig. 1. The average density $\int n_e dl / \int dl$ was approximately $1.2 \cdot 10^{19}$ m^{-3}, although some variation exists due to particle control and wall conditioning challenges.

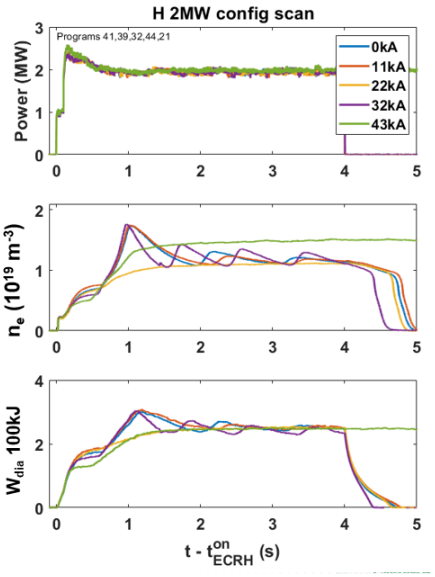

Fig. 1. Time history corresponding the SE reference discharge in the five mimic configurations.

Comparison of heat fluxes: A set of infrared (IR) cameras are used to measure the temperature of the plasma facing components (PFCs) and infer the heat flux. Data from each pixel is mapped to the PFC structure using a scene model developed from the CAD drawings, see Ref. 5 for more details. In the DIV3D simulations, a simplified representation of the full divertor geometry (see Fig. 2) is used. For

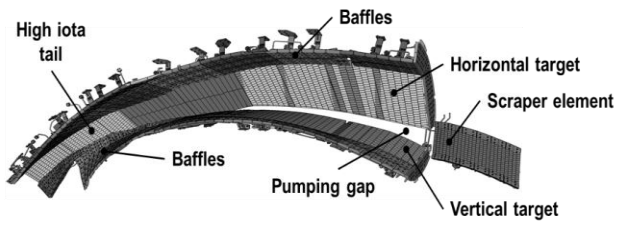

Fig. 2. Components of a W7-X divertor module.

comparison to the simulations the IR data are further mapped to the DIV3D geometry, an example is shown in Fig. 3 for a 32kA mimic configuration plasma. The pattern and relative magnitude of the IR measured temperature is well reproduced by the DIV3D calculations. The DIV3D calculations have been shown to qualitatively match the heat flux predictions from higher fidelity EMC3-EIRENE simulations [6]. This suggests that the approach of field line diffusion is appropriate for predicting the wetted areas and approximate heat fluxes for stellarator configurations and design studies.

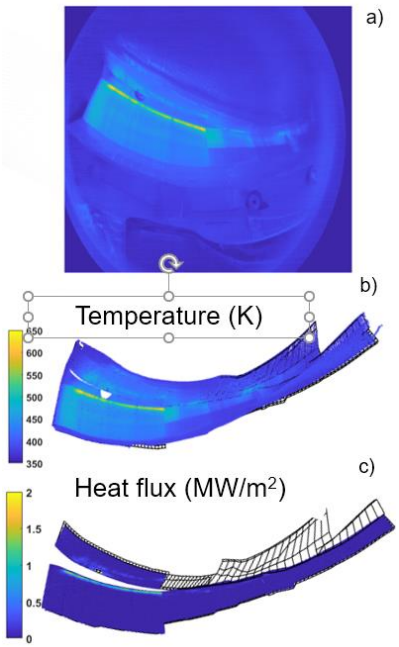

Fig 3. a) raw camera image, b) temperature mapped to DIV3D geometry, c) DIV3D heat flux for a 32kA mimic configuration plasma

For a limited number of configurations, the heat fluxes have been calculated from the IR temperature [5]. The heat fluxes have been evaluated for the horizontal and vertical targets, the high iota tail, and the connecting baffle-like components. Figure 4 shows the experimental heat fluxes and those from DIV3D using the SE design point magnetic diffusivity ($D_m = 3.155 \cdot 10^{-6}$ m^2/m) for the 0kA, 32kA, and 43kA configurations focusing on the horizontal and vertical target areas. The general agreement of the simulations and experimental data, showing the transition from a limited shape to an island diverted shape, indicates that the approach of mimicking the OP2 topology changes using the planar and control coils is valid. In each case the approximate patterns and relative magnitudes are reproduced, however some important differences can be observed. The experimental flux patterns are somewhat narrower than the DIV3D

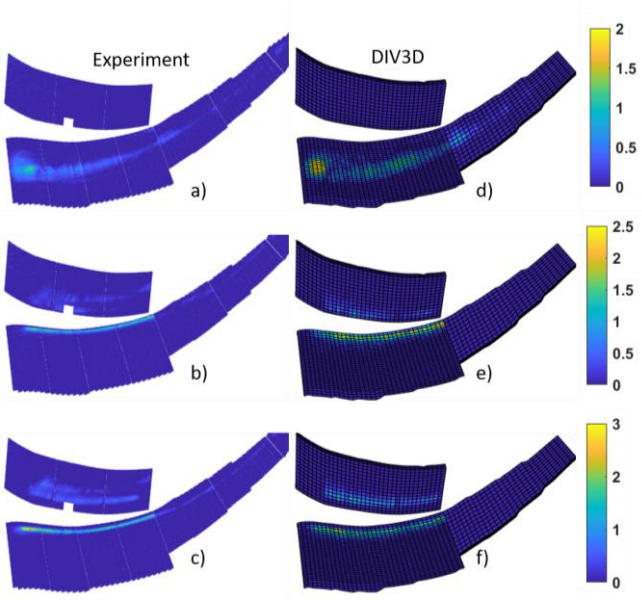

Fig 4. Experimental heat fluxes in the a) 0kA, b) 32kA, and c) 43kA configurations, and corresponding DIV3D heat fluxes (d-f) using the design point magnetic diffusivity.

simulations, indicating that the cross-field transport used in the modeling is too large. At the same time, the magnitudes are generally smaller in the DIV3D calculation, despite the larger wetted area. This is expected, as the DIV3D simulations do not include any dissipative processes such as impurity radiation. An exception to this is the 43kA configuration, where the peak heat fluxes on the horizontal target exceed those from the design point modeling. Fig. 5 shows the heat flux from experiment and a range of diffusivities in DIV3D at two toroidal locations on the horizontal plate. The value of 1/3 the design diffusivity appears to match the measured width, however it only reproduces the peak flux at one toroidal location. At the other toroidal position, the experimental flux exceeds the simulated level, however the peak flux in the modeling does not change significantly over this range. This is because the heat flux patterns at the 'front' of the divertor are from short connection length flux tubes (where the circular pattern is located in the 0kA configuration in Fig. 4) and are less sensitive to the diffusivity. The lack of agreement in this range indicates a need for higher fidelity simulations, which may better capture these trends. The 43kA configuration may show different trends due to higher density and collisionality. Calibrated data from the power and density scans (not yet available) will be used to investigate this behavior.

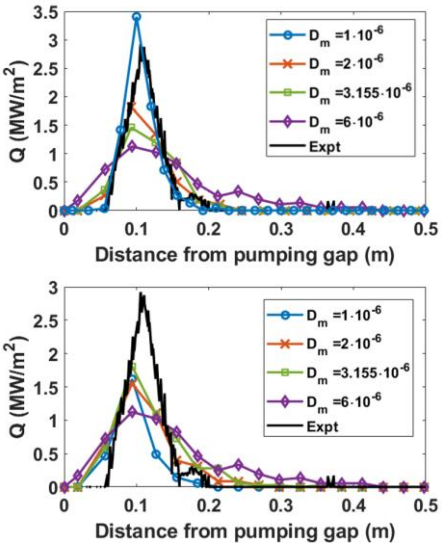

Fig. 5. Radial profiles of heat fluxes from experiment and a range of diffusivities in DIV3D for two different toroidal angles in the 43kA configuration.

Acknowledgements: This material is based upon work supported by the US Department of Energy under contract number DE-AC05-00OR22725. This work has been carried out within the framework of the EUROfusion Consortium and has received funding from the Euratom research and training programme 2014-2018 under grant agreement No 633053. The views and opinions expressed herein do not necessarily reflect those of the European Commission.

References:

[1] A. Peacock, et al., Proc. IEEE/NPSS 24th Symp. Fusion Eng., Jun. 2011, pp. 1–5.
[2] J.D. Lore, et al., IEEE TPS 42, 539 (2014).
[3] J. Geiger, et al., Contrib. Plasma Phys., 50 (2010) 770
[4] H. Hölbe, et al., Nucl. Fusion, 56, 026015, 2016.
[5] M.Jakubowski, et al., Rev. Sci. Inst. (2018), accepted for publication.
[6] J.D. Lore, et al., IEEE TPS 46 (2018) 1387.